Assessing Interactions between Helical Aromatic Oligoamide Foldamers and Protein Surfaces: A Tethering Approach

Maëlle Vallade,[†] Michal Jewginski,[†,‖] Lucile Fischer,[†] Jérémie Buratto,[†] Katell Bathany,[†] Jean-Marie Schmitter,[†] Marine Stupfel,[†] Frédéric Godde,[†] Cameron D. Mackereth,[§] and Ivan Huc[*,†,‡]

[†]Université Bordeaux, CNRS, IPB, CBMN (UMR 5248), Institut Européen de Chimie et Biologie, 2 rue Robert Escarpit, 33600 Pessac, France

[‖]Department of Bioorganic Chemistry, Faculty of Chemistry, Wrocław University of Technology, 50-370 Wrocław, Poland

[§]Université Bordeaux, INSERM, CNRS, ARNA (U 1212 and UMR 5320), Institut Européen de Chimie et Biologie, 2 rue Robert Escarpit, 33600 Pessac, France

[‡]Department Pharmazie, Ludwig-Maximilians-Universität, Butenandtstraße 5-13, D-81377 München, Germany

Ⓢ *Supporting Information*

ABSTRACT: Helically folded aromatic foldamers may constitute suitable candidates for the *ab initio* design of ligands for protein surfaces. As preliminary steps toward the exploration of this hypothesis, a tethering approach was developed to detect interactions between a protein and a foldamer by confining the former at the surface of the latter. Cysteine mutants of two therapeutically relevant enzymes, CypA and IL4, were produced. Two series of ten foldamers were synthesized bearing different proteinogenic side chains and either a long or a short linker functionalized with an activated disulfide. Disulfide exchange between the mutated cysteines and the activated disulfides yielded 20 foldamer-IL4 and 20 foldamer-CypA adducts. Effectiveness of the reaction was demonstrated by LC-MS, by MS analysis after proteolytic digestion, and by 2D NMR. Circular dichroism then revealed diastereoselective interactions between the proteins and the foldamers confined at their surface which resulted in a preferred handedness of the foldamer helix. Helix sense bias occurred sometimes with both the short and the long linkers and sometimes with only one of them. In a few cases, helix handedness preference is found to be close to quantitative. These cases constitute valid candidates for structural elucidation of the interactions involved.
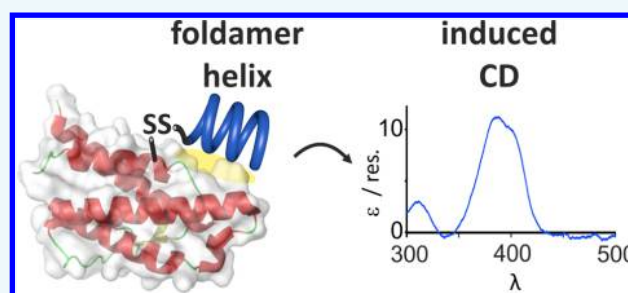
INTRODUCTION

Ligands that act as inhibitors of protein−protein or protein−nucleic acid interactions by covering large surface areas of protein surfaces may be identified using diverse strategies. Directed evolution methods such as Selex, phage display, or mRNA display have successfully delivered peptidic, proteic, or nucleotidic ligands through the iterative screening of very large libraries.[1−8] Screening of libraries of synthetic molecules is another possibility.[9−13] Structure-based design through epitope mimicry may also be considered when binding epitopes have been characterized. For example, the field of α-helix mimetics has been flourishing[14] following the realization that α-helices are common motifs at protein−protein interfaces leading to the development of linear oligo-arylamides[15−18] and arylureas,[19] as well as other linear rods,[20−24] peptides containing β-amino acids,[25−29] stapled peptides,[30−34] or α-peptide β-sheets.[35] β-Sheet mimicry[36−40] and nucleic acid mimicry[41,42] have also been considered. In contrast, except for recognition based on charge complementarity between polyanionic ligands and a polycationic protein,[43,44] we are not aware of major

advances toward the *ab initio* design of ligands for large surface areas of proteins, i.e., design (as opposed to discovery and screening) without information about what could constitute a tight binder. Such an approach would have the advantage to potentially deliver protein ligands for any desired location of a protein even when no binding epitope is known.

We have proposed that aromatic amide foldamers[45,46] might constitute appropriate scaffolds to be decorated with proteinogenic side chains to bind to, and cover, large surface areas of proteins. Aromatic amide foldamers adopt folded conformations that are both stable and predictable and that may reach sizes well above 5 kDa.[47,48] They can be prepared via solid phase synthesis (SPS)[49,50] and several strategies allow for the introduction of varied proteinogenic side chains at their surface,[51] including their combination with α-amino acids.[48,52] As first steps toward the design of protein surface ligands based

on these scaffolds, we have explored a tethering strategy that consists of confining a foldamer at the surface of a protein to investigate foldamer−protein interactions even when binding may be weak.[53−56] This strategy is reminiscent of other approaches in which tethering was exploited, e.g., in fragment-based screening by dynamic combinatorial libraries,[13] or for the stepwise elongation of ligands.[57−61] The concept of tethering has also been applied to investigate protein−protein interactions (PPIs) in less stable complexes.[62,63] We initially used human carbonic anhydrase (HCAII) as a model system and noncovalent ligation as the tethering method. HCAII is stable, commercially available, and easy to crystallize. In addition, simple and readily available aromatic sulfonamides bind to its active site with nanomolar affinity. Thus, different tetrameric and pentameric helical foldamers derived from 8-amino-2-quinolinecarboxylic acid were prepared, functionalized with an HCAII ligand and confined at the surface of the protein upon ligand binding to the active site. Significant foldamer−protein interactions were detected in several cases, as these give rise to induced circular dichroism (CD) when the handedness of the helix is biased through diastereoselective interactions with stereogenic centers at the protein surface.[53−55] When CD was strong, foldamer−protein complexes were amenable to structural characterization both in the solid state by X-ray crystallography and in solution. These structures constitute valuable starting points for further design of the foldamer and the creation of selective interactions with the protein surface. Ultimately, the objective is that foldamer−-protin interactions become strong enough for binding to occur in the absence of the tether. Recently, this approach was successfully extended to a 14mer foldamer that covers a considerable surface area of HCAII.[56]

In this manuscript, we present the extension of this approach to two proteins, namely, cyclophilin A (CypA) and interleukin 4 (IL4), involved in PPIs that may constitute relevant therapeutic targets. Since these proteins do not possess active sites or known small molecule ligands, tethering consisted of covalently ligating foldamers at a cysteine residue introduced via site-directed mutagenesis using either short or long linkers (Figure 1a). We have appended active disulfides at the N-terminus of aromatic oligoamide foldamers on solid phase, optimized conditions under which foldamer-protein disulfide bridges form, and developed methods to purify these adducts and characterize them by NMR and mass spectrometry. CD revealed multiple cases in which a preferred right-handed (*P*) or left-handed (*M*) helix sense was induced in the foldamer helix, indicating selective foldamer−protein interactions. This occurred sometimes both with a short linker (i.e., when the foldamer position is somewhat constrained), with a long linker (i.e., when the foldamer is allowed to explore a larger patch of protein surface), and sometimes with one linker type only. Altogether, our results constitute an important milestone toward the identification of aromatic foldamer−protein interactions and toward the structure elucidation of foldamer−protein interfaces in the contexts of CypA and IL4.

RESULTS AND DISCUSSION

Protein Mutant Design and Production. Our choice of IL4 and CypA as targets was guided by their medium size, their structural differences (the former is α-helix rich whereas the latter is β-sheet rich, Figure 1b), and by the fact that the 3D structures of both native IL4 and CypA and their interactions with their respective partners have been structurally charac-
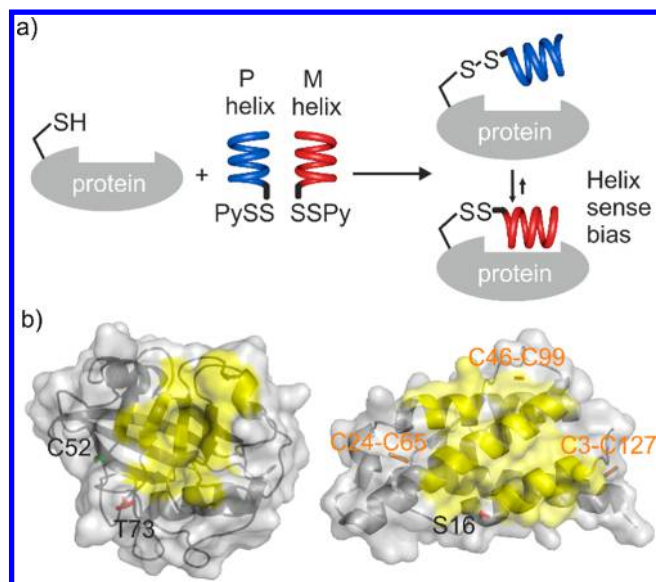

Figure 1. (a) Tethering of a racemic mixture of *P*- and *M*-helical foldamers to a protein via a disulfide bridge formation and selection of one helix handedness through diastereoselective foldamer/protein surface interactions. Py stands for 2-pyridyl. (b) Wild type proteins targeted in this study: CypA (left) and IL4 (right). The surfaces of CypA and IL4 involved in known interactions, i.e., with cyclosporin A and IL4Rα (Receptor Rα), respectively, are shown in yellow. Sites considered for targeted mutagenesis are shown in black and existing disulfide bridges in orange.

terized by X-ray crystallography and NMR spectroscopy, as well as by using mutated binding epitopes.[64−68] Thus, all residues exposed to water and in particular those involved in PPIs have been identified in both cases. Furthermore, IL4 and CypA are both therapeutically relevant. The cytokine IL4 is a major mediator of the T-helper immune response involved in proliferation and differentiation of activated cells[69] and can thus constitute a key factor in immune disorders such as allergy and inflammation. CypA is a *cis−trans* prolyl isomerase that belongs to the immunophilin family and is involved in various cellular functions including protein folding, trafficking, assembly, immunomodulation, and cell signaling. It is believed that an increase in Cyclophilin A expression contributes to pathological conditions and thus constitutes a key player for human diseases[70] including HIV infection.[71]

One mutation site to display a cysteine residue was considered on each protein near the area involved in PPIs. The sites had to be accessible at the surface, and the mutation should not change or destabilize the protein structure. IL4 has three disulfide bridges and no free cysteine. S16 is located at the surface of the protein in the vicinity of the IL4 receptor (IL4Rα) binding site. Fortunately, the recombinant expression of the S16C mutant in *E. coli* has been described previously,[72] and shown to be successful despite the potential interference of the new cysteine with the disulfide bridges. We thus opted for this mutation site to tether foldamers. Following the reported procedure,[72] IL4 S16C was produced as an insoluble protein. To protect the free thiol present at the protein surface, extracted muteins from the inclusion bodies were refolded in the presence of glutathione. Glutathionylated IL4 S16C is thus isolated. Enzymatic deglutathionylation with glutaredoxin followed by size exclusion chromatography (SEC) purification

was performed just before tethering of foldamers to C16 to avoid oxidation at this site and dimerization of the protein.
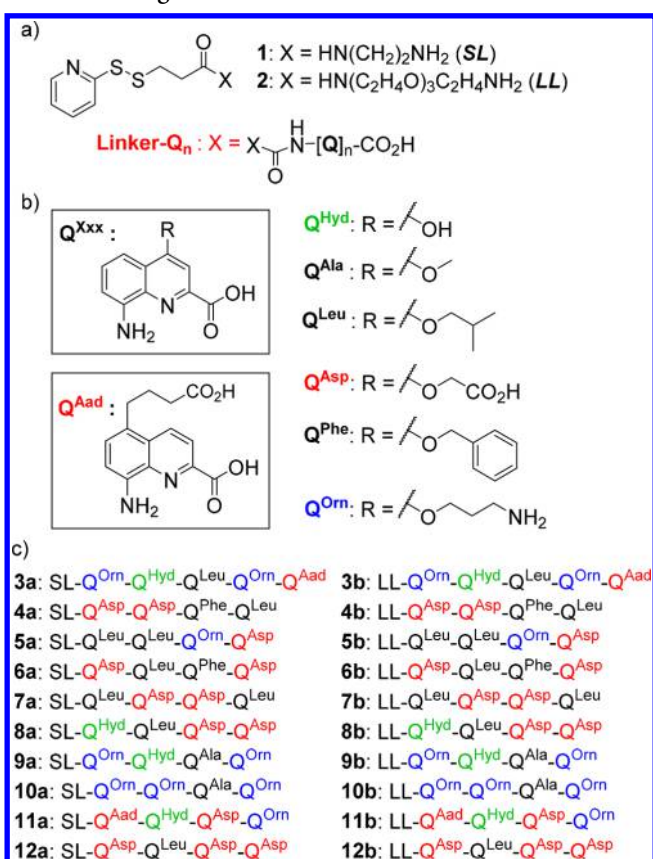
CypA has no disulfide bridge and its four cysteine residues seemed at first glance to be buried enough not to react with an active disulfide in solution. We considered T73 as a mutation site located near the CD147 binding area which is also in close proximity to the site of interaction with the natural inhibitor cyclosporin.[67,73,74] However, tethering attempts on CypA T73C showed that reactions could also take place at C52 (see below). A double mutant CypA C52A T73C in which C52 is replaced by alanine was thus considered in a second step (Figure 1b). A synthetic CypA gene was acquired with codon optimization for expression in *E. coli* in order to improve protein yields. Recombinant expression followed reported procedures.[75] The solvent exposed C73 is kept in the reduced state upon the addition of dithiothreitol (DTT). Removal of DTT with a desalting gel filtration column was performed just before foldamer tethering in order to prevent oxidation and dimerization of the protein. Bacterial expression of CypA C52A T73C was also carried out in a medium containing ^{15}N-labeled ammonium to produce isotopically-enriched proteins suitable for multidimensional NMR spectroscopic analysis.

Different experiments were carried out to check the structural integrity of both protein mutants. An enzymatic digestion of IL4 S16C was performed with trypsin. This degradation preserves disulfide bridges. The resulting peptides were identified by LC-MS. The peaks carrying the expected disulfide bridges were identified as well as the peptide carrying the mutated residue (Figure S1) showing the proper folding of the protein. Peptides containing mismatched disulfides were only seen as trace amounts. In the case of CypA, we first assigned the backbone ^{1}H,^{13}C,^{15}N nuclei of wild-type CypA in order to annotate the ^{1}H,^{15}N-HSQC spectrum (Figure S2). For CypA C52A T73C, ^{15}N-labeling enabled the fast measurement of a ^{1}H^{15}N HSQC 2D NMR spectrum that showed that the mutant adopts the same fold as wildtype CypA. The good resolution of the NMR peaks is preserved and the signals assigned to the mutated residues C52 and T73 residues have disappeared (Figure S3).

Foldamer Design and Synthesis. In order to anchor the foldamers to protein surfaces at cysteine residues, an activated disulfide was introduced at the N-terminus of foldamer sequences (Chart 1a). Disulfide exchange with the cysteine releases 2-(1H)-thiopyridone to yield a protein-foldamer disulfide. A short linker (1) and a long oligoethylene glycol linker (2) were designed in order to assess whether one fares better than the other. A short linker may in principle achieve a better confinement of the foldamer at the protein surface and enforce diastereoselective interactions. With a long linker, the foldamer possesses more conformational freedom, but it can also explore interactions with a larger surface area of the protein around the anchor point. It has thus more chances to find a spot where interactions are significant.

The synthesis of the Boc-protected precursors of the two linkers is shown in Scheme 1. A common intermediate was prepared from the reaction of commercially available 2,2′-dithiopyridine and 3-mercaptopropionic acid. The resulting 3-(2-pyridyldithio)-propionic acid acid 13 was then coupled to N-Boc-ethylenediamine to give the Boc protected short linker 14. For the long linker, the tosylate functions of commercially available tetraethylene glycol ditosylate were converted into azido groups before mono reduction of an azide and subsequent protection of the resulting amine with a Boc
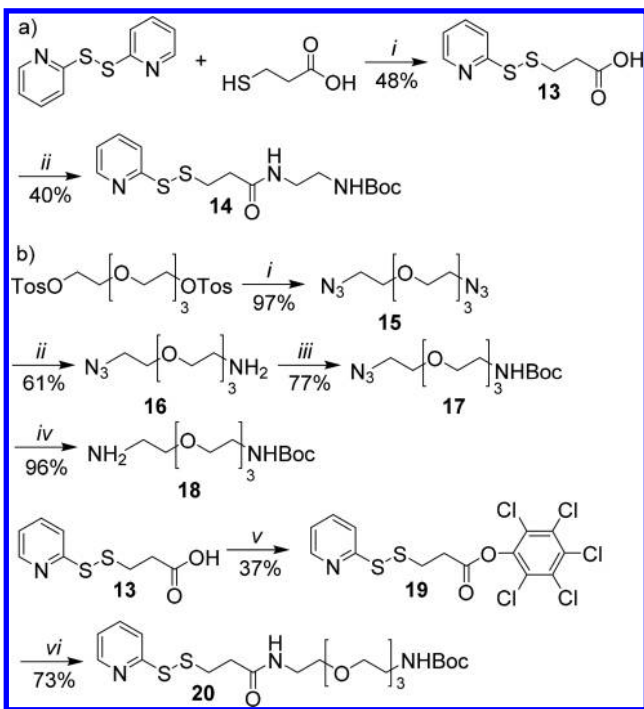
Chart 1. Design of Foldamers[a]

[a](a) linker part; (b) functionalized quinoline building blocks having hydrophobic (black), polar (green), positively charged (blue), negatively charged (red) residues; (c) list of the sequences synthesized.

group at one extremity. The reduction of the remaining azido group yielded amine 18 that was coupled to the pyridyldithiopropionic acid 13 activated as a pentachlorophenyl carbonate to give Boc protected long linker 20. The Boc protecting groups were removed from the linker precursors with TFA prior to use. Attachment of the aliphatic amine of linkers 1 and 2 to the N-terminal aromatic amine of a quinoline oligoamide chain on the solid phase was carried out as for HCAII ligands.[53] The terminal 8-aminoquinoline was activated as an isocyanate directly on the Wang resin by triphosgene. Amine 1 or 2 were then added to form a urea (Chart 1a).

Foldamers were prepared using quinoline monomers functionalized with proteinogenic side chains in position 4 or 5. Side chains attached in these positions diverge from helices. Monomers are designated Q^{Xxx} using the Xxx three-letter code of analogous α-amino acids when available (Chart 1b). Fmoc-Q^{Xxx} monomers have been previously described[50,53] except Fmoc-Q^{Aad} acid whose synthesis will be reported elsewhere. Side chain acid and amine functions were protected as acid labile *tert*-butyl ester or *tert*-butyloxycarbonyl (Boc), respectively.

To screen different foldamers for their interactions with the surface of both proteins, two series of ten sequences were prepared by SPS,[76] bearing the short or long linker, respectively (Chart 1c). No design was introduced other than to create a certain degree of sequence diversity within

Scheme 1. (a) Synthesis of Boc protected short linker: (*i*) AcOH, MeOH, 25 °C, N₂; (*ii*) N-Boc-ethylenediamine, HATU, DIEA, THF, 25 °C; (b) Synthesis of Boc protected long linker: (*i*) NaN₃, DMF, 65 °C; (*ii*) PPh₃, Et₂O/THF/ HCl 1 M, 25 °C; (*iii*) Boc₂O, CH₂Cl₂, 0 °C then 25 °C; (*iv*) H₂, Pd/C, AcOEt, 25 °C; (*v*) pentachlorophenol, EDC.HCl, DMAP, THF, 25 °C; (*vi*) **18**, Et₃N, THF, 25 °C

were added in order to ensure completion of the reaction and avoid the presence of uncoupled protein. Assuming that foldamer binding and CD induction without tethering is a rare event, the remaining untethered foldamer in solution may not affect the CD results as it will remain a racemic mixture of *P* and *M* helices. Foldamers are not all readily soluble in water and were added to the protein from 2 mM DMSO stock solutions. Proteins were dissolved in an aqueous 50 mM NaCl 10 mM TRIS buffer at pH 7.5. These conditions favor disulfide exchange and preserve protein folding. Tethering proceeds within 1 h at room temperature. Samples are then let at 4 °C until further analyses are performed. For the purpose of structural studies, the same conditions may be applied on a larger scale. Excess foldamer was removed by semipreparative reverse HPLC in the case of IL4-foldamer adducts, or using centrifugal filters in the case of CypA-foldamer adducts.

Several techniques were used to demonstrate protein-foldamer-adduct formation. LC-MS analysis can be carried out on the crude reaction sample (Figure 2). The tethered
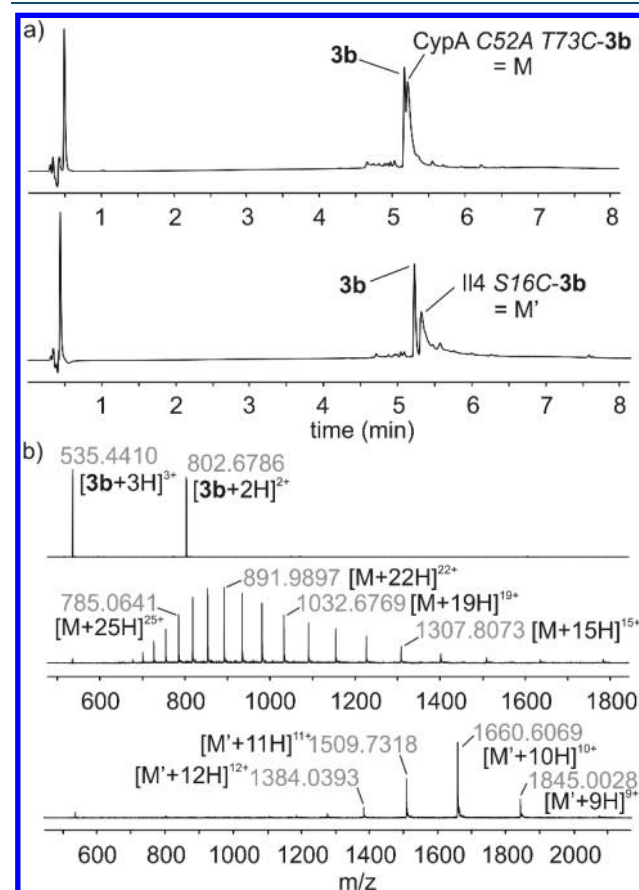

Figure 2. (a) UV traces (λ = 360 nm) of the LC-MS analysis of protein/foldamer **3b** adducts with CypA *C52AT73C* (top) and IL4 *S16C* (bottom). (b) Mass spectra of HPLC peaks of excess **3b** (top), CypA *C52AT73C*-**3b** adduct M (middle) and IL4 *S16C*-**3b** adduct M′ (bottom).

oligomers four or five units long using six different hydrophobic, neutral polar, cationic, or anionic side chains. Crude oligomers are typically obtained in 50−90% purity. Side chain deprotection and cleavage from the resin was carried out in 95:2.5:2.5 TFA/*i*Pr₃SiH/H₂O (vol/vol/vol). Sequences were purified by reversed-phase HPLC and obtained in 7−70% yield from initial Wang resin loadings. The choice of side chains of **3a**−**12b** was intended to be diverse. Most sequences carry a mix of charged and hydrophobic residues: the goal was to generate small libraries with no special bias for any particular residue. Importantly, sequences **3a**−**12b** do not carry any stereogenic center and thus exist as a mixture of *P* and *M* enantiomeric helical conformers. Q*ₙ* sequences were kept short (4 to 5 residues) to allow helix handedness inversion to occur in solution. Indeed, helix stability rises so quickly upon increasing oligomer length[77] that longer sequences do not undergo any equilibrium in protic media.[78] Nevertheless, fast dynamics can be induced in these sequences upon combining Q*^{Xxx}* monomers with more flexible units.[56]

Tethering of Foldamers to Protein Surfaces. This was considered in two distinct contexts. For the purpose of screening interactions, reactions should be carried out on small scales to consume as little mutant protein and foldamer as possible. Purification may not be necessary. Conversely, for structural studies, several milligrams of purified adducts may be needed. In this study, we considered circular dichroism in 2 mm cuvettes as a means to probe foldamer−protein interactions. This typically required a 300 μL sample of a 20 μM foldamer-protein adduct solution for each foldamer. Typically, 2 equiv of foldamer bearing an activated disulfide

protein as well as the excess foldamer are easily detected at 360 nm due to the high absorbance of quinoline rings. The mass spectra of the corresponding peaks ascertain purity. The entire consumption of the uncoupled protein and completion of the reaction can be monitored at 280 nm (not shown). For both IL4 *S16C* and CypA *C52A T73C*, the chromatograms show no trace of multiple adducts demonstrating that ligation does not

alter the other disulfide bridges (IL4) and buried cysteines (CypA).

NMR was used to monitor chemical shift variations that result from tethering the Boc-protected short linker **14** on ^{15}N labeled CypA and CypA *C52A T73C* (Figure 3). With native
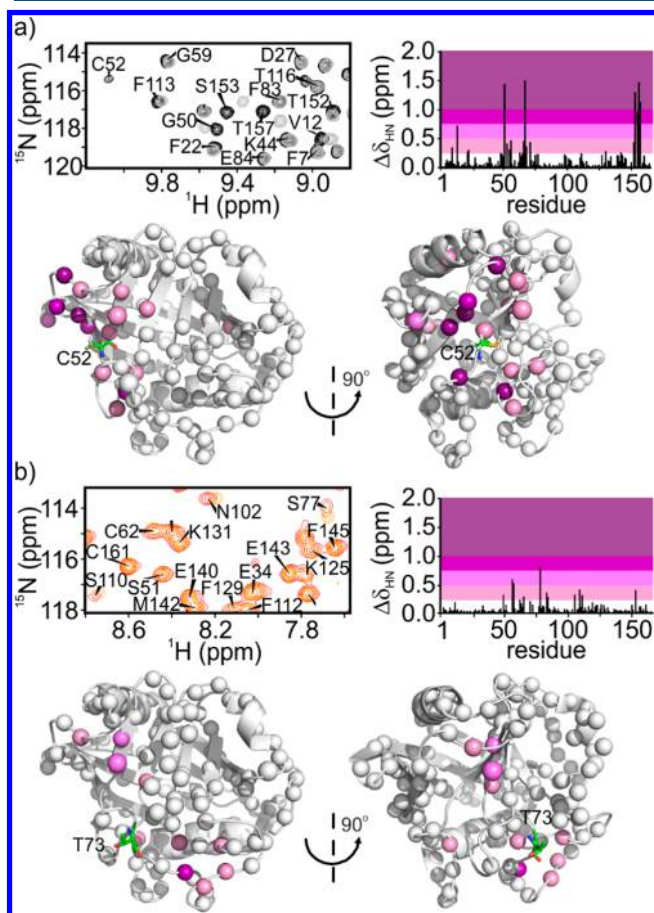

Figure 3. Ligation of Boc-protected short linker **14** to (a) CypA, top left: overlay of ^{1}H^{15}N HSQC for CypA (black) and CypA-**14** (gray); top right: $\Delta\delta_{HN}$ of CypA-**14** compared to CypA, calculated as the root-mean-square deviation, $((\Delta\delta_H/0.14)^2 + (\Delta\delta_N)^2)^{0.5}$;[79] bottom: each observed amide nitrogen atom in the ^{1}H^{15}N HSQC is represented as a sphere on the structure of CypA (PDB ID: 1wca)[74] and colored as in top right; (b) CypA *C52AT73C*, top left: overlay of ^{1}H^{15}N HSQC for CypA *C52AT73C* (red) and CypA *C52AT73C*-**14** (orange); top right: $\Delta\delta_{HN}$ of CypA *C52AT73C*-**14** compared to CypA *C52AT73C*, calculated as in (a); bottom: each observed amide nitrogen atom in the ^{1}H^{15}N HSQC is represented as a sphere on the structure of CypA (PDB ID: 1wca)[74] and colored as in top right.

CypA, chemical shift variations were observed in the vicinity of C52 showing that the reaction took place at this site, hence the necessity of the *C52A* mutation. With the double *C52A T73C* mutant, chemical shift variations were observed as expected in the vicinity of C73 that can be reached by the tethered linker. The ^{15}N HSQC spectra also demonstrated that the proteins remain well folded after attachment of the short linker, and that tethering is quantitative.

For IL4 *S16C*, tethering of long linker-foldamer **3b** was investigated by MS analysis after trypsin digestion (Figure 4a) of the HPLC purified adduct. The peptides resulting from the digestion were analyzed by LC-MS. At 360 nm, peptides do not absorb and only the foldamer-containing peptides are seen
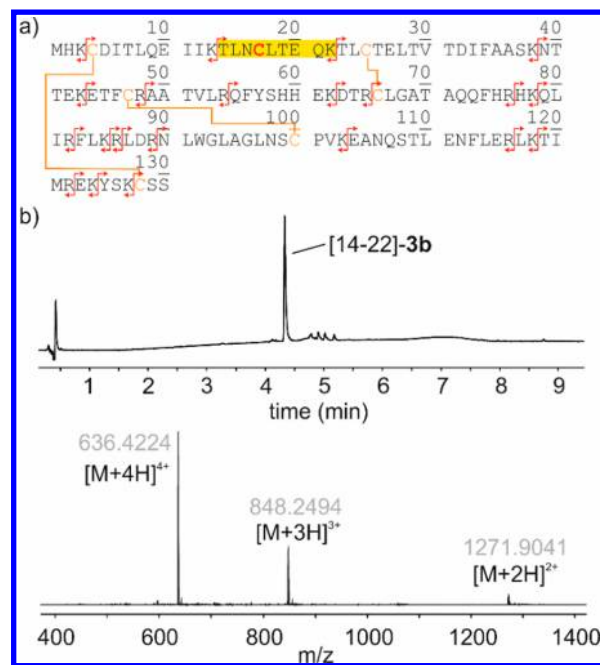

Figure 4. Tryptic digestion of the adduct between **3b** and IL4 *S16C*. (a) Amino-acid sequence of the mutant protein with cleavage sites (red arrows), peptide containing the mutated residue C16 (yellow) and native disulfide bridges (orange); (b) LC-MS profile of the digested sample of the adduct showing the characteristic peak (λ = 360 nm) of the peptide [14−22] bearing the foldamer moiety of **3b** (top) and the corresponding mass profile (bottom).

(Figure 4b). This allowed to confirm that ligation takes place at C16. HPLC nevertheless reveals small amounts of foldamer attachment at other sites, although it is not clear whether this occurred before digestion, or after through disulfide exchange (see also Figure S4).

Assessment of Foldamer−Protein Interactions by CD. CD was used as a screening method in order to detect interactions between the two series of ten foldamers and the surface of the two protein mutants. The spectra normalized per residue are shown in Figure 5. Remarkably, almost half of the foldamer sequences give rise to a non-negligible CD signal. It should be pointed out here that the small library of foldamers described in this study represent all of the tested sequences. No sequence has been discarded and the high frequency of significant handedness induction is thus representative. For some foldamers (e.g., **5a**-CypA or **6b**-IL4) signal intensity is quite high. Based on earlier studies of one-handed helices,[80] this intensity indicates near to complete handedness induction. Many of the foldamers display interactions with both proteins, others with only one (e.g., **4b**-IL4, **6a**-CypA, **8a**-CypA, and **12a**-CypA). At the notable exception of **6b**-IL4, it is remarkable that foldamers all show a preference for *P*-handedness at the surface of IL4 and for *M*-handedness at the surface of CypA. Such a prevalence over numerous sequences can hardly be a coincidence and may reflect interactions between the protein and the main chain of the foldamer. The differences observed between the various foldamer sequences would then be the outcome of interactions involving foldamer side-chains. At this stage of the study, we have no means to tell whether some protein structural changes are involved upon interacting with the foldamer, as has been described with other proteins.[81] Nevertheless, CypA and IL4
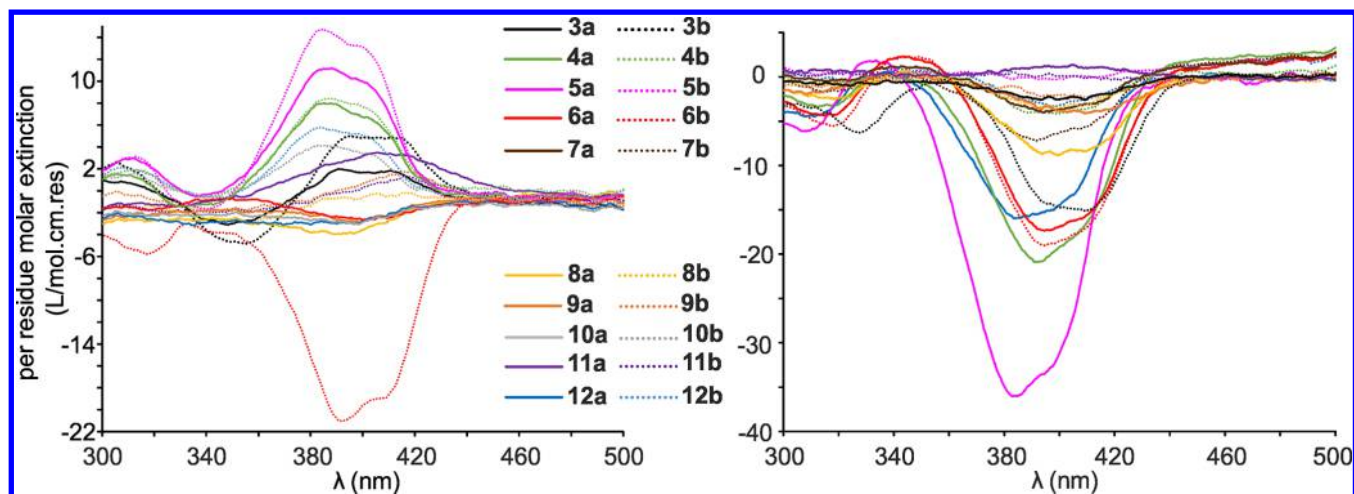
Figure 5. Induced CD spectra of protein/foldamer adducts with IL4 *S16C* (left) and Cyp A *C52AT73C* (right). Experiments have been carried out with crude samples containing 20 μM protein-adducts in 10 mM TRIS buffer and 50 mM NaCl, pH 7.5.

(which possesses several disulfide bridges) are known to have quite stable structures.

Intense CD signals are observed with both short and long linkers, but there is no correlation between the two: in some cases, a tethered foldamer sequence may give rise to an intense CD signal with both a short and a long linker (e.g., **4a**/**4b**-IL4, **5a**/**5b**-IL4, **9a**/**9b**-CypA), but in other cases only the short linker (**5a**-CypA, **12a**-CypA) or only the long linker (**6b**-IL4) gave rise to an intense CD. This shows that different patches of the protein surface may be involved according to linker length and that screening both linkers is a worthy investment as both bring their own advantages.

In some cases a shift of the wavelength of the maximal CD intensity is observed. This may be due to the monomer composition. For example red-shifts are observed with **3a**, **3b**, **11a**, and **11b**. These contain not only 4-substituted monomers but also 5-substituted monomer Q^{Aad} which absorbs at longer wavelengths. However, the blue shift of **5a**-CypA might be the reflection of a particular foldamer conformation.

CONCLUSION

In conclusion, we have validated methods to covalently tether a variety of helically folded aromatic oligoamide sequences to cysteine residues introduced by site-directed mutagenesis at the surface of two therapeutically relevant proteins, IL4 and CypA. Different analytical methods confirm the effective ligation by formation of a disulfide bridge, even in the presence of other protein disulfide bridges in the case of IL4, and in the presence of buried free cysteine residues for CypA. CD then allowed the detection of diastereoselective foldamer–protein interactions resulting in a preferred helix handedness in the foldamer. This validates CD as an efficient tool to screen these interactions. CD spectra also validated the interest of testing both short and long linkers between the protein and the foldamer. In a few cases, intense CD bands hint at stronger foldamer–protein interactions. This invites an assessment of the binding affinity and selectivity in the absence of linker. Preliminary results indicate that handedness induction indeed sometimes occurs even when the foldamer is not covalently linked to the protein. These cases constitute suitable candidates for a scaled-up production of the adducts to attempt structural investigations, in particular, crystal growth for the purpose of X-ray crystallographic analysis as was previously achieved in the case of noncovalent attachment to HCAII.[53−56] Steps are currently being made toward these objectives and will be reported in due course.

ASSOCIATED CONTENT

Ⓢ Supporting Information
The Supporting Information is available free of charge on the ACS Publications website at DOI: 10.1021/acs.bioconjchem.8b00710.

> Tryptic digestion experiments, 2D NMR experiments, detailed experimental methods, and analytical data for new compounds (PDF)

AUTHOR INFORMATION

Corresponding Author
*E-mail: ivan.huc@cup.lmu.de.
ORCID ⓘ
Cameron D. Mackereth: 0000-0002-0776-7947
Ivan Huc: 0000-0001-7036-9696
Notes
The authors declare no competing financial interest.

ACKNOWLEDGMENTS

REFERENCES

(1) Packer, M. S., and Liu, D. R. (2015) Methods for the directed evolution of proteins. *Nat. Rev. Genet. 16*, 379−394. Lane, M. D., and Seelig, B. (2014) Advances in the directed evolution of proteins. *Curr. Opin. Chem. Biol. 22*, 129−136.

(2) Lao, Y.-H., Phua, K. K. L., and Leong, K. W. (2015) Aptamer nanomedicine for cancer therapeutics: barriers and potential for translation. *ACS Nano 9*, 2235−2254.

(3) Pande, J., Szewczyk, M. M., and Grover, A. K. (2010) Phage display: concept, innovations, applications and future. *Biotechnol. Adv. 28*, 849−858.

(4) Wilson, D. R., and Finlay, B. B. (1998) Phage display: applications, innovations, and issues in phage and host biology. *Can. J. Microbiol. 44*, 313−329.

(5) Sidhu, S. S., Lowman, H. B., Cunningham, B. C., and Wells, J. A. (2000) Phage display for selection of novel binding peptides. *Methods Enzymol. 328*, 333−363.

(6) Koivunen, E., Arap, W., Rajotte, D., Lahdenranta, J., and Pasqualini, R. (1999) Identification of receptor ligands with phage display peptide libraries. *J. Nucl. Med. 40* (5), 883−888.

(7) Rami, A., Behdani, M., Yardehnavi, N., Habibi-Anbouhi, M., and Kazemi-Lomedasht, F. (2017) An overview on application of phage display technique in immunological studies. *Asian Pac. J. Trop. Biomed. 7*, 599−602.

(8) Wilson, D. S., Keefe, A. D., and Szostak, J. W. (2001) The use of MRNA display to select high-affinity protein-binding peptides. *Proc. Natl. Acad. Sci. U. S. A. 98*, 3750−3755.

(9) Hebda, J. A., Magzoub, M., and Miranker, A. D. (2014) Small molecule screening in context: Lipid-catalyzed amyloid formation. *Protein Sci. 23*, 1341−1348.

(10) Kumar, S., Schlamadinger, D. E., Brown, M. A., Dunn, J. M., Mercado, B., Hebda, J. A., and Miranker, A. D. (2015) Islet amyloid-induced cell death and bilayer integrity loss share a molecular origin targetable with oligopyridylamide-based α-helical mimetics. *Chem. Biol. 22*, 369−378.

(11) Kumar, S., Birol, M., and Miranker, A. D. (2016) Foldamer scaffolds suggest distinct structures are associated with alternative gains-of-function in a preamyloid toxin. *Chem. Commun. 52*, 6391−6394.

(12) Choi, S., and Choi, K.-Y. (2017) Screening-based approaches to identify small molecules that inhibit protein−protein interactions. *Expert Opin. Drug Discovery 12*, 293−303.

(13) Arkin, M. R., Randal, M., DeLano, W. L., Hyde, J., Luong, T. N., Oslob, J. D., Raphael, D. R., Taylor, L., Wang, J., McDowell, R. S., et al. (2003) Binding of small molecules to an adaptive protein−protein interface. *Proc. Natl. Acad. Sci. U. S. A. 100*, 1603−1608.

(14) Wilson, A. J. (2015) Helix mimetics: Recent developments. *Prog. Biophys. Mol. Biol. 119*, 33−40. Jayatunga, M. K. P., Thompson, S., and Hamilton, A. D. (2014) α-Helix mimetics: Outwards and upwards. *Bioorg. Med. Chem. Lett. 24*, 717−724.

(15) Ernst, J. T., Becerril, J., Park, H. S., Yin, H., and Hamilton, A. D. (2003) Design and application of an α-helix-mimetic scaffold based on an oligoamide-foldamer strategy: antagonism of the Bak BH3/Bcl-xL complex. *Angew. Chem., Int. Ed. 42*, 535−539.

(16) Plante, J. P., Burnley, T., Malkova, B., Webb, M. E., Warriner, S. L., Edwards, T. A., and Wilson, A. J. (2009) Oligobenzamide proteomimetic inhibitors of the p53−hDM2 protein−protein interaction. *Chem. Commun.*, 5091−5093.

(17) Ahn, J.-M., and Han, S.-Y. (2007) Facile synthesis of benzamides to mimic an α-helix. *Tetrahedron Lett. 48*, 3543−3547.

(18) Shaginian, A., Whitby, L. R., Hong, S., Hwang, I., Farooqi, B., Searcey, M., Chen, J., Vogt, P. K., and Boger, D. L. (2009) Design, synthesis, and evaluation of an α-helix mimetic library targeting protein−protein interactions. *J. Am. Chem. Soc. 131*, 5564−5572.

(19) Rodriguez, J. M., and Hamilton, A. D. (2007) Benzoylurea oligomers: synthetic foldamers that mimic extended α helices. *Angew. Chem., Int. Ed. 46*, 8614−8617.

(20) Yin, H., Lee, G., Park, H. S., Payne, G. A., Rodriguez, J. M., Sebti, S. M., and Hamilton, A. D. (2005) Terphenyl-based helical mimetics that disrupt the p53/HDM2 interaction. *Angew. Chem., Int. Ed. 44*, 2704−2707.

(21) Anderson, L., Zhou, M., Sharma, V., McLaughlin, J. M., Santiago, D. N., Fronczek, F. R., Guida, W. C., and McLaughlin, M. L.

(2010) Facile iterative synthesis of 2,5-terpyrimidinylenes as non-peptidic α-helical mimics. *J. Org. Chem. 75*, 4288−4291.

(22) Perato, S., Fogha, J., Sebban, M., Voisin-Chiret, A. S., Sopkova-de Oliveira Santos, J., Oulyadi, H., and Rault, S. (2013) Conformation control of abiotic α-helical foldamers. *J. Chem. Inf. Model. 53*, 2671−2680.

(23) Raghuraman, A., Ko, E., Perez, L. M., Ioerger, T. R., and Burgess, K. (2011) Pyrrolinone−pyrrolidine oligomers as universal peptidomimetics. *J. Am. Chem. Soc. 133*, 12350−12353.

(24) Xin, D., Perez, L. M., Ioerger, T. R., and Burgess, K. (2014) A multifaceted secondary structure mimic based on piperidine-piperidinones. *Angew. Chem., Int. Ed. 53*, 3594−3598.

(25) Cheng, R. P., Gellman, S. H., and DeGrado, W. F. (2001) β-Peptides: from structure to function. *Chem. Rev. 101*, 3219−3232.

(26) Sadowsky, J. D., Fairlie, W. D., Hadley, E. B., Lee, H.-S., Umezawa, N., Nikolovska-Coleska, Z., Wang, S., Huang, D. C. S., Tomita, Y., and Gellman, S. H. (2007) (α/β+α)-peptide antagonists of BH3 domain/Bcl-xl recognition: toward general strategies for foldamer-based inhibition of protein−protein interactions. *J. Am. Chem. Soc. 129*, 139−154.

(27) Pilsl, L. K. A., and Reiser, O. (2011) α/β-Peptide foldamers: state of the art. *Amino Acids 41*, 709−718.

(28) Sawada, T., and Gellman, S. H. (2011) Structural mimicry of the α-helix in aqueous solution with an isoatomic α/β/γ-peptide backbone. *J. Am. Chem. Soc. 133*, 7336−7339.

(29) Grison, C. M., Miles, J. A., Robin, S., Wilson, A. J., and Aitken, D. J. (2016) An α-helix-mimicking 12,13-helix: designed α/β/γ-foldamers as selective inhibitors of protein−protein interactions. *Angew. Chem., Int. Ed. 55*, 11096−11100.

(30) Walensky, L. D., Kung, A. L., Escher, I., Malia, T. J., Barbuto, S., Wright, R. D., Wagner, G., Verdine, G. L., and Korsmeyer, S. J. (2004) Activation of apoptosis in vivo by a hydrocarbon-stapled BH3 helix. *Science 305*, 1466−1470.

(31) Chang, Y. S., Graves, B., Guerlavais, V., Tovar, C., Packman, K., To, K.-H., Olson, K. A., Kesavan, K., Gangurde, P., Mukherjee, A., et al. (2013) Stapled α−helical peptide drug development: A potent dual inhibitor of MDM2 and MDMX for p53-dependent cancer therapy. *Proc. Natl. Acad. Sci. U. S. A. 110*, 3445−3454.

(32) Cromm, P. M., Spiegel, J., and Grossmann, T. N. (2015) Hydrocarbon stapled peptides as modulators of biological function. *ACS Chem. Biol. 10*, 1362−1375.

(33) Grison, C. M., Burslem, G. M., Miles, J. A., Pilsl, L. K. A., Yeo, D. J., Imani, Z., Warriner, S. L., Webb, M. E., and Wilson, A. J. (2017) Double quick, double click reversible peptide "stapling". *Chem. Sci. 8*, 5166−5171.

(34) Hack, V., Reuter, C., Opitz, R., Schmieder, P., Beyermann, M., Neudörfl, J.-M., Kühne, R., and Schmalz, H.-G. (2013) Efficient α-helix induction in a linear peptide chain by N-capping with a bridged-tricyclic diproline analogue. *Angew. Chem., Int. Ed. 52*, 9539−9543.

(35) Fasan, R., Dias, R. L. A., Moehle, K., Zerbe, O., Vrijbloed, J. W., Obrecht, D., and Robinson, J. A. (2004) Using a β-hairpin to mimic an α-helix: cyclic peptidomimetic inhibitors of the p53−HDM2 protein−protein interaction. *Angew. Chem., Int. Ed. 43*, 2109−2112.

(36) Khakshoor, O., Demeler, B., and Nowick, J. S. (2007) Macrocyclic beta-sheet peptides that mimic protein quaternary structure through intermolecular beta-sheet interactions. *J. Am. Chem. Soc. 129*, 5558−5569.

(37) Jamieson, A. G., Russell, D., and Hamilton, A. D. (2012) A 1,3-phenyl-linked hydantoin oligomer scaffold as a β-strand mimetic. *Chem. Commun. 48*, 3709−3711.

(38) German, E. A., Ross, J. E., Knipe, P. C., Don, M. F., Thompson, S., and Hamilton, A. D. (2015) β-strand mimetic foldamers rigidified through dipolar repulsion. *Angew. Chem., Int. Ed. 54*, 2649−2652.

(39) Jouanne, M., Voisin-Chiret, A.-S., Legay, R., Coufourier, S., Rault, S., and Sopkova-de Oliveira Santos, J. (2016) β-strand mimicry: exploring oligothienylpyridine foldamers. *Eur. J. Org. Chem. 2016*, 5686−5696.

(40) Zerbe, K., Moehle, K., and Robinson, J. A. (2017) Protein epitope mimetics: from new antibiotics to supramolecular synthetic vaccines. *Acc. Chem. Res. 50*, 1323−1331.

(41) Yüksel, D., Bianco, P. R., and Kumar, K. (2016) De novo design of protein mimics of B-DNA. *Mol. BioSyst. 12*, 169−177.

(42) Ziach, K., Chollet, C., Parissi, V., Prabhakaran, P., Marchivie, M., Corvaglia, V., Bose, P. P., Laxmi-Reddy, K., Godde, F., Schmitter, J.-M., et al. (2018) Single helically folded aromatic oligoamides that mimic the charge surface of double-stranded B-DNA. *Nat. Chem. 10*, 511−518.

(43) Hamuro, Y., Crego Calama, M., Park, H. S., and Hamilton, A. D. (1997) A calixarene with four peptide loops: an antibody mimic for recognition of protein surfaces. *Angew. Chem., Int. Ed. Engl. 36*, 2680−2683.

(44) McGovern, R. E., Fernandes, H., Khan, A. R., Power, N. P., and Crowley, P. B. (2012) Protein camouflage in cytochrome C-calixarene complexes. *Nat. Chem. 4*, 527−533.

(45) Huc, I. (2004) Aromatic oligoamide foldamers. *Eur. J. Org. Chem. 2004*, 17−29.

(46) Zhang, D.-W., Zhao, X., Hou, J.-L., and Li, Z.-T. (2012) Aromatic amide foldamers: structures, properties, and functions. *Chem. Rev. 112*, 5271−5316.

(47) Delsuc, N., Massip, S., Léger, J.-M., Kauffmann, B., and Huc, I. (2011) Relative helix−helix conformations in branched aromatic oligoamide foldamers. *J. Am. Chem. Soc. 133*, 3165−3172.

(48) De, S., Chi, B., Granier, T., Qi, T., Maurizot, V., and Huc, I. (2017) Designing cooperatively folded abiotic uni- and multi-molecular helix bundles. *Nat. Chem. 10*, 51−57.

(49) Murphy, N. S., Prabhakaran, P., Azzarito, V., Plante, J. P., Hardie, M. J., Kilner, C. A., Warriner, S. L., and Wilson, A. J. (2013) Solid-phase methodology for synthesis of O-alkylated aromatic oligoamide inhibitors of α-helix-mediated protein−protein interactions. *Chem. - Eur. J. 19*, 5546−5550.

(50) Hu, X., Dawson, S. J., Nagaoka, Y., Tanatani, A., and Huc, I. (2016) Solid-phase synthesis of water-soluble helically folded hybrid α-amino acid/quinoline oligoamides. *J. Org. Chem. 81*, 1137−1150.

(51) Hu, X., Dawson, S. J., Mandal, P. K., de Hatten, X., Baptiste, B., and Huc, I. (2017) Optimizing side chains for crystal growth from water: a case study of aromatic amide foldamers. *Chem. Sci. 8*, 3741−3749.

(52) Kudo, M., Maurizot, V., Kauffmann, B., Tanatani, A., and Huc, I. (2013) Folding of a linear array of α-amino acids within a helical aromatic oligoamide frame. *J. Am. Chem. Soc. 135*, 9628−9631.

(53) Buratto, J., Colombo, C., Stupfel, M., Dawson, S. J., Dolain, C., Langlois d'Estaintot, B., Fischer, L., Granier, T., Laguerre, M., Gallois, B., et al. (2014) Structure of a complex formed by a protein and a helical aromatic oligoamide foldamer at 2.1 Å resolution. *Angew. Chem., Int. Ed. 53*, 883−887.

(54) Jewginski, M., Fischer, L., Colombo, C., Huc, I., and Mackereth, C. D. (2016) Solution observation of dimerization and helix handedness induction in a human carbonic anhydrase−helical aromatic amide foldamer complex. *ChemBioChem 17*, 727−736.

(55) Jewginski, M., Granier, T., Langlois d'Estaintot, B., Fischer, L., Mackereth, C. D., and Huc, I. (2017) Self-assembled protein−aromatic foldamer complexes with 2:3 and 2:2:1 stoichiometries. *J. Am. Chem. Soc. 139*, 2928−2931.

(56) Vallade, M., Reddy, S. P., Fischer, L., and Huc, I. (2018) Enhancing aromatic foldamer helix dynamics to probe interactions with protein surfaces. *Eur. J. Org. Chem. 2018*, 5489−5498.

(57) Jain, A., Whitesides, G. M., Alexander, R. S., and Christianson, D. W. (1994) Identification of two hydrophobic patches in the active-site cavity of human carbonic anhydrase II by solution-phase and solid-state studies and their use in the development of tight-binding inhibitors. *J. Med. Chem. 37*, 2100−2105.

(58) Andersson, T., Lundquist, M., Dolphin, G. T., Enander, K., Jonsson, B.-H., Nilsson, J. W., and Baltzer, L. (2005) The binding of human carbonic anhydrase II by functionalized folded polypeptide receptors. *Chem. Biol. 12*, 1245−1252.

(59) Banerjee, A. L., Swanson, M., Roy, B. C., Jia, X., Haldar, M. K., Mallik, S., and Srivastava, D. K. (2004) Protein surface-assisted enhancement in the binding affinity of an inhibitor for recombinant human carbonic anhydrase-II. *J. Am. Chem. Soc. 126*, 10875−10883.

(60) Enander, K., Dolphin, G. T., and Baltzer, L. (2004) Designed, functionalized helix−loop−helix motifs that bind human carbonic anhydrase II: a new class of synthetic receptor molecules. *J. Am. Chem. Soc. 126*, 4464−4465.

(61) Schulze Wischeler, J., Sun, D., Sandner, N. U., Linne, U., Heine, A., Koert, U., and Klebe, G. (2011) Stereo- and regioselective azide/alkyne cycloadditions in carbonic anhydrase II via tethering, monitored by crystallography and mass spectrometry. *Chem. - Eur. J. 17*, 5842−5851.

(62) Cigler, M., Müller, T. G., Horn-Ghetko, D., von Wrisberg, M.-K., Fottner, M., Goody, R. S., and Lang, K. (2017) Proximity-triggered covalent stabilization of low-affinity protein complexes in vitro and in vivo. *Angew. Chem., Int. Ed. 56*, 15737−15741.

(63) Yang, B., Tang, S., Ma, C., Li, S.-T., Shao, G.-C., Dang, B., and Wang, L. (2017) Spontaneous and specific chemical cross-linking in live cells to capture and identify protein interactions. *Nat. Commun. 8*, 2240.

(64) For IL-4: (a) Wlodaver, A., Pavlovsky, A., and Gustchina, A. (1992) Crystal structure of human recombinant interleukin-4 at 2.25 Å resolution. *FEBS Lett. 309*, 59−64.

(65) Zhang, J.-L., Simeonowa, I., Wang, Y., and Sebald, W. (2002) The high-affinity interaction of human IL-4 and the receptor α chain is constituted by two independent binding clusters. *J. Mol. Biol. 315*, 399−407.

(66) For cyclophilin A: (a) Ke, H., Zydowsky, L. D., Liu, J., and Walsh, C. T. (1991) Crystal structure of recombinant human T-cell cyclophilin A at 2.5 Å resolution. *Proc. Natl. Acad. Sci. U. S. A. 88*, 9483−9487.

(67) Schlegel, J., Redzic, J. S., Porter, C. C., Yurchenko, V., Bukrinsky, M., Labeikovsky, W., Armstrong, G. S., Zhang, F., Isern, N. G., DeGregori, J., et al. (2009) Solution characterization of the extracellular region of CD147 and its interaction with its enzyme ligand cyclophilin A. *J. Mol. Biol. 391*, 518−535.

(68) Yurchenko, V., Zybarth, G., O'Connor, M., Dai, W. W., Franchin, G., Hao, T., Guo, H., Hung, H.-C., Toole, B., Gallay, P., et al. (2002) Active site residues of cyclophilin A are crucial for its signaling activity via CD147. *J. Biol. Chem. 277*, 22959−22965.

(69) Malek, T. R. (2008) The biology of interleukin-2. *Annu. Rev. Immunol. 26*, 453−479.

(70) Nigro, P., Pompilio, G., and Capogrossi, M. C. (2013) Cyclophilin A: a key player for human disease. *Cell Death Dis. 4*, e888.

(71) Liu, C., Perilla, J. R., Ning, J., Lu, M., Hou, G., Ramalho, R., Himes, B. A., Zhao, G., Bedwell, G. J., Byeon, I.-J., et al. (2016) Cyclophilin A stabilizes the HIV-1 capsid through a novel noncanonical binding site. *Nat. Commun. 7*, 10714.

(72) Duppatla, V., Gjorgjevikj, M., Schmitz, W., Kottmair, M., Mueller, T. D., and Sebald, W. (2012) Enzymatic deglutathionylation to generate interleukin-4 cysteine muteins with free thiol. *Bioconjugate Chem. 23*, 1396−1405.

(73) Kallen, J., Spitzfaden, C., Zurini, M. G. M., Wider, G., Widmer, H., Wüthrich, K., and Walkinshaw, M. D. (1991) Structure of human cyclophilin and its binding site for cyclosporin A determined by X-ray crystallography and NMR spectroscopy. *Nature 353*, 276−279.

(74) Mikol, V., Kallen, J., Pflügl, G., and Walkinshaw, M. D. (1993) X-ray structure of a monomeric cyclophilin A-cyclosporin A crystal complex at 2·1 Å resolution. *J. Mol. Biol. 234*, 1119−1130.

(75) Liu, J., Albers, M. W., Chen, C. M., Schreiber, S. L., and Walsh, C. T. (1990) Cloning, expression, and purification of human cyclophilin in Escherichia coli and assessment of the catalytic role of cysteines by site-directed mutagenesis. *Proc. Natl. Acad. Sci. U. S. A. 87*, 2304−2308.

(76) Dawson, S. J., Hu, X., Claerhout, S., and Huc, I. (2016) Solid phase synthesis of helically folded aromatic oligoamides. *Methods Enzymol. 580*, 279−301.

(77) Delsuc, N., Kawanami, T., Lefeuvre, J., Shundo, A., Ihara, H., Takafuji, M., and Huc, I. (2008) Kinetics of helix-handedness inversion: folding and unfolding in aromatic amide oligomers. *ChemPhysChem 9*, 1882−1890.

(78) Qi, T., Maurizot, V., Noguchi, H., Charoenraks, T., Kauffmann, B., Takafuji, M., Ihara, H., and Huc, I. (2012) Solvent dependence of helix stability in aromatic oligoamide foldamers. *Chem. Commun. 48*, 6337−6339.

(79) Williamson, M. P. (2013) Using chemical shift perturbation to characterise ligand binding. *Prog. Nucl. Magn. Reson. Spectrosc. 73*, 1−16.

(80) Kendhale, A. M., Poniman, L., Dong, Z., Laxmi-Reddy, K., Kauffmann, B., Ferrand, Y., and Huc, I. (2011) Absolute control of helical handedness in quinoline oligoamides. *J. Org. Chem. 76*, 195−200.

(81) Kumar, S., Birol, M., Schlamadinger, D. E., Wojcik, S. P., Rhoades, E., and Miranker, A. D. (2016) Foldamer-mediated manipulation of a pre-amyloid toxin. *Nat. Commun. 7*, 11412.